Supplementary Information
Universal constraint on nonlinear population dynamics

Kyosuke Adachi,[1,2] Ryosuke Iritani,[2,3] and Ryusuke Hamazaki[4,2]

[1]*Nonequilibrium Physics of Living Matter RIKEN Hakubi Research Team, RIKEN Center for Biosystems Dynamics Research (BDR), 2-2-3 Minatojima-minamimachi, Chuo-ku, Kobe 650-0047, Japan*

[2]*RIKEN Interdisciplinary Theoretical and Mathematical Sciences Program (iTHEMS), 2-1 Hirosawa, Wako 351-0198, Japan*

[3]*Department of Biological Sciences, Graduate School of Science, University of Tokyo, 7-3-1 Hongo, Bunkyo-ku, Tokyo 113-0033, Japan*

[4]*Nonequilibrium Quantum Statistical Mechanics RIKEN Hakubi Research Team, RIKEN Cluster for Pioneering Research (CPR), 2-1 Hirosawa, Wako 351-0198, Japan*

(Dated: May 1, 2022)

Supplementary Method 1: Price equation and speed-limit inequality

Purely from the conservation of the total proportion, $\sum_{i=1}^{L} P_i = 1$, we can derive the Price equation [1, 2],

$$\partial_t \langle A \rangle = \mathrm{cov}(A, \partial_t P/P) + \langle \partial_t A \rangle . \tag{1}$$

Here, $A := \{A_i\}_{i=1}^{L}$ is a generally time-dependent quantity depending on each type, e.g., the growth rate, $\langle A \rangle := \sum_{i=1}^{L} P_i A_i$, $\mathrm{cov}(A, B) := \langle (A - \langle A \rangle)(B - \langle B \rangle) \rangle$, and $\partial_t P/P := \{\partial_t P_i / P_i\}_{i=1}^{L}$.

We define the speed of A as $v_A := |\partial_t \langle A \rangle - \langle \partial_t A \rangle| / \Delta A$ [3, 4] with $\Delta A := \sqrt{\langle (A - \langle A \rangle)^2 \rangle}$. The inverse of the speed, ${v_A}^{-1}$, represents the time required for A to change to a statistically distinguishable value [4], and thus v_A characterizes the speed of the temporal change in A [Fig. 1(a)]. From Supplementary Eq. (1), we obtain the speed-limit inequality [Eq. (3)] as

$$\begin{aligned} v_A &= \frac{|\mathrm{cov}(A, \partial_t P/P)|}{\Delta A} \\ &\leq \frac{1}{\Delta A} \sqrt{\sum_{i=1}^{L} P_i (A_i - \langle A \rangle)^2} \sqrt{\sum_{i=1}^{L} P_i \left(\frac{\partial_t P_i}{P_i} \right)^2} \\ &= \sqrt{\langle (\partial_t P/P)^2 \rangle}, \end{aligned}$$

where $\langle \partial_t P/P \rangle = \partial_t \sum_{i=1}^{L} P_i = 0$ and the Cauchy-Schwarz inequality are used in the second line.

The equal sign in Eq. (3) is achieved when $A - \langle A \rangle$ is parallel or anti-parallel to $\partial_t P/P$ in the L-dimensional vector space, where $\partial_t P_i / P_i$ is regarded as the ith component of $\partial_t P/P$, for instance. This means that the speed of A is faster as the correlation between A and the instantaneous growth rate is stronger. When there are only two types ($L = 2$), we can explicitly obtain $(A_1 - \langle A \rangle, A_2 - \langle A \rangle) = (A_1 - A_2)(P_2, -P_1)$ and $(\partial_t P_1/P_1, \partial_t P_2/P_2) = [\partial_t P_1/(P_1 P_2)](P_2, -P_1)$, leading to $(A - \langle A \rangle) \parallel \partial_t P/P$, and the equal sign in Eq. (3) is achieved regardless of the details of dynamics.

Supplementary Method 2: Fisher's fundamental theorem of natural selection

We first take $F_i = s_i N_i$ in Eq. (1), where $s_i > 0$ is the type-dependent growth rate. Since $\partial_t P_i = (s_i - \langle s \rangle) P_i$ from Eq. (2), Supplementary Eq. (1) leads to

$$\partial_t \langle s \rangle = \mathrm{cov}(s, s - \langle s \rangle) = (\Delta s)^2, \tag{2}$$

which means that the rate of increase in the average growth rate is equal to the variance of the growth rate, known as Fisher's fundamental theorem of natural selection [5–11]. On the other hand, the equation $\partial_t P_i = (s_i - \langle s \rangle) P_i$ also leads to $v_{\mathrm{lim}} = [\langle (s - \langle s \rangle)^2 \rangle]^{1/2} = \Delta s$. Since $v_s = |\partial_t \langle s \rangle| / \Delta s$ by definition, Supplementary Eq. (2) is equivalent to $v_s = v_{\mathrm{lim}}$, suggesting that Fisher's fundamental theorem is nothing but a special case of Eq. (3).

If we explicitly solve the equation $\partial_t P_i = (s_i - \langle s \rangle) P_i$, the solution is given by the following softmax function:

$$P_i(t) = \frac{P_i(0) \exp(s_i t)}{\sum_{j=1}^{L} P_j(0) \exp(s_j t)}. \tag{3}$$

Conversely, if the time-dependent proportion is the same type of softmax function as Supplementary Eq. (3), we can obtain the saturation of the speed ($v_s = v_{\mathrm{lim}}$).

We next take $F_i = f_i(\{N_i\}_{i=1}^L, t)N_i$ in Eq. (1) with an arbitrary function f_i, which is the so-called fitness [12] and represents the growth rate that can depend on the effects of interactions among types. From Eq. (2) and Supplementary Eq. (1), we obtain $\partial_t \langle f \rangle - \langle \partial_t f \rangle = (\Delta f)^2$, which is known as an extended version of Fisher's fundamental theorem [12, 13]. Since we can obtain $v_{\rm lim} = \Delta f$ and $v_f = |\partial_t \langle f \rangle - \langle \partial_t f \rangle| / \Delta f$ in the same way as explained above, the extended version of the fundamental theorem is equivalent to a special case of Eq. (3), $v_f = v_{\rm lim}$.

Supplementary Method 3: Evolutionary model with natural selection and mutation

We take $F_i = s_i N_i + \sum_{j=1}^L m_{ij} N_j$ in Eq. (1) [14, 15], where $s_i > 0$ is the growth rate, $m_{ij} \geq 0$ ($i \neq j$) is the mutation rate from type j to i, and $\sum_{i=1}^L m_{ij} = 0$ for all j. Note that m_{ij} is related to the mutation probability Q_{ij} from j to i [16, 17], which satisfies $\sum_{i=1}^L Q_{ij} = 1$, as $m_{ij} = Q_{ij} s_j$ (for $i \neq j$) and $m_{jj} = (Q_{jj} - 1)s_j$. Also note that here we consider a large and well-mixed population which can be approximated by assuming that the size is infinite and that noise [18] and spatial effects are zero [16]. In the following, we further assume $s_i = \bar{s} + r\delta_{i1}$ ($\bar{s}, r > 0$), $m_{1j} = 0$ for $j \neq 1$, and $m_{ij} > 0$ for $i \neq 1$ and $i \neq j$, where δ_{ij} is the Kronecker delta. From Eq. (2), we can obtain the equation for P_1 as $\partial_t P_1 = (r + m_{11} - rP_1)P_1$. Thus, $r_{\rm c}$ ($:= -m_{11} = \sum_{i=2}^L m_{i1}$) is a transcritical bifurcation point [19]: $P_1^{\rm s} = 0$ for $r \leq r_{\rm c}$, while $P_1^{\rm s} = (r - r_{\rm c})/r > 0$ for $r > r_{\rm c}$, provided $P_1(t = 0) > 0$, where $P_i^{\rm s} := P_i(t \to \infty)$ is the steady-state proportion of type i. The qualitative change in $P_1^{\rm s}$ at $r = r_{\rm c}$ represents the transition between survival and extinction of type 1.

At the bifurcation point ($r = r_{\rm c}$), P_1 satisfies

$$\partial_t P_1 = -r_{\rm c} {P_1}^2, \tag{4}$$

which leads to $P_1 \sim t^{-1}$ after a long time. If a quantity A is independent of time, e.g., $A = s$ (growth rate) or $A = b$ (type index), we can obtain $\partial_t \langle A \rangle \sim t^{-2}$ according to $P_1 \sim t^{-1}$. Then, assuming that ΔA shows a power-law decay as $\Delta A \sim t^{-\delta_A}$ with a certain exponent δ_A, we obtain $v_A = |\partial_t \langle A \rangle| / \Delta A \sim t^{-2+\delta_A}$. On the other hand, if A is time-dependent, e.g., $A = I = -\ln P$ (diversity), the asymptotic time dependence of $\partial_t \langle A \rangle - \langle \partial_t A \rangle$, ΔA, and $v_A = |\partial_t \langle A \rangle - \langle \partial_t A \rangle| / \Delta A$ generally depends on the time dependence of A. Thus, the asymptotic forms of the speeds follow $v_s \sim t^{-3/2}$ since $\Delta s = [P_1(1 - P_1)]^{1/2} r_{\rm c} \sim t^{-1/2}$ (i.e., $\delta_s = 1/2$), $v_b \sim t^{-2}$ since $\Delta b(t \to \infty) \neq 0$ (i.e., $\delta_b = 0$), and $v_I \sim t^{-2} \ln t$ since $|\partial_t \langle I \rangle - \langle \partial_t I \rangle| \sim t^{-2} \ln t$ and $\Delta I(t \to \infty) \neq 0$.

Near but off the bifurcation point ($r \simeq r_{\rm c}$), we can linearize the equation of P_1 after a long time as

$$\partial_t (P_1 - P_1^{\rm s}) \simeq -|r - r_{\rm c}|(P_1 - P_1^{\rm s}), \tag{5}$$

both for $r > r_{\rm c}$ and $r < r_{\rm c}$. Thus, P_1 shows an exponential relaxation with the relaxation time proportional to $|r - r_{\rm c}|^{-1}$, which diverges at the bifurcation point. Such divergence suggests that the relaxation times τ_A (for v_A) and $\tau_{\rm lim}$ (for $v_{\rm lim}$) should also diverge at the bifurcation point as $\tau_A \sim |r - r_{\rm c}|^{-\beta_A}$ and $\tau_{\rm lim} \sim |r - r_{\rm c}|^{-\beta_{\rm lim}^{\rm TC}}$ with certain exponents β_A and $\beta_{\rm lim}^{\rm TC}$. This motivates us to consider the dynamical scaling laws [Eq. (6) and Eq. (7)] since similar dynamical scaling is applied to order parameters with diverging relaxation time in critical phenomena [20, 21]. Since the inequality [Eq. (3)] indicates that v_A should show an exponential decay earlier than $v_{\rm lim}$, we obtain an inequality between the relaxation timescales as $\tau_A \leq \tau_{\rm lim}$ near the bifurcation point, which leads to $\beta_A \leq \beta_{\rm lim}^{\rm TC}$.

For Figs. 2, 3(a)-(c), Supplementary Figs. 1, and 2, we used the mutation rates

$$(m_{ij}) = \begin{pmatrix} -2.1 & 0 & 0 \\ 1 & -1.2 & 0.8 \\ 1.1 & 1.2 & -0.8 \end{pmatrix}$$

with $r_{\rm c} = -m_{11} = 2.1$ and the initial state $(P_1, P_2, P_3)|_{t=0} = (0.2, 0.5, 0.3)$.

Supplementary Method 4: SIR model with birth and death

We take $L = 3$, $F_1 = 1 - \lambda N_1 N_2 / N_{\rm tot} - N_1$, $F_2 = \lambda N_1 N_2 / N_{\rm tot} - \gamma N_2 - N_2$, and $F_3 = \gamma N_2 - N_3$ in Eq. (1), where N_1, N_2, and N_3 are the densities of susceptible, infected, and recovered individuals, respectively [22]. Here, λ is the infection rate, γ is the recovery rate, and we take both the birth and death rates as unity by rescaling time t and $N_{\rm tot}$, where the death rate is assumed to be the same for all three types. Assuming a nonzero proportion of the infected individuals at the initial time [$P_2(t = 0) > 0$], we can obtain the steady-state proportions as

$$(P_1^{\rm s}, P_2^{\rm s}, P_3^{\rm s}) = \begin{cases} (1, 0, 0) & (\lambda \leq \lambda_{\rm c}) \\ \left(\frac{\lambda_{\rm c}}{\lambda}, \frac{\lambda - \lambda_{\rm c}}{\lambda_{\rm c} \lambda}, \frac{(\lambda_{\rm c} - 1)(\lambda - \lambda_{\rm c})}{\lambda_{\rm c} \lambda} \right) & (\lambda > \lambda_{\rm c}) \end{cases},$$

where the extinction transition for the infected and recovered individuals occurs through the transcritical bifurcation at $\lambda = \lambda_{\rm c}$ ($:= \gamma + 1$).

We consider the long-time dynamics of N_i at the bifurcation point ($\lambda = \lambda_{\rm c}$). First, since $N_{\rm tot}$ shows an exponential relaxation according to $\partial_t N_{\rm tot} = 1 - N_{\rm tot}$, $N_{\rm tot} \simeq 1$ after a long time. Defining the deviation from the steady state as $\Delta N_i := N_i - N_i^{\rm s}$ with

$(N_1^{\rm s}, N_2^{\rm s}, N_3^{\rm s}) := (1, 0, 0)$, we can linearize Eq. (1) as $\partial_t \Delta N_1 = -\Delta N_1 - \lambda_{\rm c} \Delta N_2$, $\partial_t \Delta N_2 = 0$, and $\partial_t \Delta N_3 = -\Delta N_3 + (\lambda_{\rm c} - 1)\Delta N_2$. These linearized equations suggest that N_1 and N_3 should adiabatically follow the dynamics of N_2, which is expected to show a power-law decay if nonlinearity is taken into account. Thus, we apply the adiabatic approximation ($\partial_t N_1 \simeq 0$) to the equation for N_1 and obtain $N_1 \simeq (1 + \lambda_{\rm c} N_2/N_{\rm tot})^{-1} \simeq (1 + \lambda_{\rm c} N_2)^{-1}$ on the timescale where N_2 changes. Then, $\partial_t N_2 = \lambda_{\rm c}(N_1/N_{\rm tot} - 1)N_2 \simeq -{\lambda_{\rm c}}^2 {N_2}^2 + O({N_3}^3)$, leading to a power-law decay of N_2 as expected: $N_2 \simeq ({\lambda_{\rm c}}^2 t)^{-1}$. Lastly, applying the adiabatic approximation ($\partial_t N_3 \simeq 0$) to the equation for N_3, we obtain $N_3 \simeq (\lambda_{\rm c} - 1)N_2 \simeq (\lambda_{\rm c} - 1)({\lambda_{\rm c}}^2 t)^{-1}$. In terms of the proportion, $P_2 \sim P_3 \sim t^{-1}$ is followed. Regarding the power-law decay of the speed of change in diversity, we obtain $v_I \sim t^{-3/2}$ since $|\partial_t \langle I \rangle - \langle \partial_t I \rangle| = |\sum_i (\partial_t P_i) \ln P_i| \sim t^{-2} \ln t$ and $\Delta I = [\sum_i P_i (\ln P_i)^2 - (\sum_i P_i \ln P_i)^2]^{1/2} \sim t^{-1/2} \ln t$.

For Fig. 3(d) and Supplementary Fig. 3, we used the recovery rate $\gamma = 15$, the infection rate $\lambda = \lambda_{\rm c} = 16$, and the initial state $(N_1, N_2, N_3)|_{t=0} = (1.1, 0.1, 0)$.

Supplementary Method 5: Power-law decay at the supercritical Hopf bifurcation

The normal form of the supercritical Hopf bifurcation is given as $\partial_t z = (\mu + {\rm i}\omega) z - |z|^2 z$, where z is a complex variable and $\omega > 0$ [19]. The only fixed point is $z = 0$ for $\mu \leq 0$, while the limit cycle appears with the amplitude $|z| = \sqrt{\mu}$ and the period $2\pi/\omega$ for $\mu > 0$. At the bifurcation point ($\mu = 0$), the amplitude follows $\partial_t |z| = -|z|^3$, which leads to a power-law decay of the amplitude as $|z| \sim t^{-1/2}$ and correspondingly an oscillatory decay of ${\rm Re}\, z$ or ${\rm Im}\, z$ as $\sim t^{-1/2} \cos \omega t$.

Supplementary Method 6: Competitive Lotka-Volterra model

We take $F_i = s_i N_i - \sum_{j=1}^{L} c_{ij} N_i N_j$ in Eq. (1), where s_i is the growth rate, and $c_{ij} > 0$ represents the competitive interaction between type i and j [23]. Using the previously obtained bifurcation diagram [24] as a reference, we take $L = 3$, $(s_1, s_2, s_3) = (19, 3/2, 12)$, and

$$(c_{ij}) = \begin{pmatrix} 1 & 2 & 4 \\ c_{21} & 1/6 & 1/3 \\ 1 & 1 & 3 \end{pmatrix}.$$

Within a certain range of c_{21} and initial states, the limit cycle appears for $c_{21} < c_{\rm c}$, while the steady-state coexistence of three types appears for $c_{21} \geq c_{\rm c}$, where $c_{\rm c}$ is the supercritical Hopf bifurcation point, and the numerically found value is $c_{\rm c} = 0.064163908$.

We used $c_{21} = 0.063833$ for Figs. 4(a) and (b), $c_{21} = c_{\rm c}$ for Fig. 4(c) and Supplementary Fig. 4, and $0.999 c_{\rm c} \leq c \leq 1.001 c_{\rm c}$ for Fig. 4(d) and Supplementary Fig. 5, with the initial state $(N_1, N_2, N_3)|_{t=0} = (20, 5, 2)$. To solve the differential equations [Eq. (1)], we used a Julia package DifferentialEquations.jl [25].

Supplementary Method 7: Power-law decay at the saddle-node bifurcation

The normal form of the saddle-node bifurcation is given as $\partial_t x = \mu - x^2$, where the stable fixed point ($x = \sqrt{\mu}$) appears only for $\mu > 0$ [19]. At the bifurcation point ($\mu = 0$), we can obtain a power-law decay as $x \sim t^{-1}$.

Considering a population dynamics that undergoes the saddle-node bifurcation as an abrupt change in the density and proportion of type 1, we should obtain $P_1 \sim {\rm const.} + t^{-1}$ at the bifurcation point for a certain range of initial states. Then, the speed limit will follow $v_{\rm lim} = [\sum_i (\partial_i P_i)^2 / P_i]^{1/2} \sim t^{-\alpha_{\rm lim}^{\rm SN}}$ with $\alpha_{\rm lim}^{\rm SN} = 2$.

Supplementary References

[1] G. R. Price, Extension of covariance selection mathematics, Ann. Hum. Genet. **35**, 485 (1972).
[2] S. A. Frank and F. J. Bruggeman, The fundamental equations of change in statistical ensembles and biological populations, Entropy **22**, 1395 (2020).
[3] S. Ito and A. Dechant, Stochastic time evolution, information geometry, and the cramér-rao bound, Phys. Rev. X **10**, 021056 (2020).
[4] S. B. Nicholson, L. P. García-Pintos, A. del Campo, and J. R. Green, Time–information uncertainty relations in thermodynamics, Nat. Phys. **16**, 1211 (2020).
[5] C. C. Li, Fundamental theorem of natural selection, Nature **214**, 505 (1967).
[6] G. R. Price, Fisher's 'fundamental theorem' made clear, Ann. Hum. Genet. **36**, 129 (1972).
[7] S. A. Frank and M. Slatkin, Fisher's fundamental theorem of natural selection, Trends Ecol. Evol. **7**, 92 (1992).
[8] S. A. Frank, Natural selection maximizes fisher information, J. Evol. Biol. **22**, 231 (2009).
[9] A. Grafen, Biological fitness and the fundamental theorem of natural selection, Am. Nat. **186**, 1 (2015).
[10] A. Grafen, Biological fitness and the price equation in class-structured populations, J. Theor. Biol. **373**, 62 (2015).
[11] A. Grafen, The left hand side of the fundamental theorem of natural selection, J. Theor. Biol. **456**, 175 (2018).
[12] J. C. Baez, The fundamental theorem of natural selection, Entropy **23**, 1436 (2021).
[13] A. W. F. Edwards, The fundamental theorem of natural selection, Biol. Rev. **69**, 443 (1994).
[14] J. J. Bull, L. A. Meyers, and M. Lachmann, Quasispecies made simple, PLOS Comput. Biol. **1**, 1 (2005).
[15] E. Domingo and C. Perales, Viral quasispecies, PLoS Genet. **15**, 1 (2019).
[16] C. O. Wilke, Quasispecies theory in the context of population genetics, BMC Evol. Biol. **5**, 44 (2005).
[17] W. F. Basener and J. C. Sanford, J. Math. Biol. **76**, 1589 (2018).
[18] W. Basener, S. Cordova, O. Hössjer, and J. Sanford, Dynamical systems and fitness maximization in evolutionary biology, in *Handbook of the Mathematics of the Arts and Sciences*, edited by B. Sriraman (Springer International Publishing, Cham, 2020) pp. 1–72.

[19] S. H. Strogatz, *Nonlinear Dynamics and Chaos with Student Solutions Manual: With Applications to Physics, Biology, Chemistry, and Engineering* (CRC Press, 2018).
[20] B. Schmittmann and R. Zia, *Statistical Mechanics of Driven Diffusive System*, edited by C. Domb and J. Lebowitz, Phase Transitions and Critical Phenomena, Vol. 17 (Academic Press, 1995).
[21] M. Henkel, H. Hinrichsen, and S. Lübeck, *Non-Equilibrium Phase Transitions, Vol. I: Absorbing Phase Transitions* (Springer, 2008).
[22] M. Kretzschmar and J. Wallinga, Mathematical models in infectious disease epidemiology, in *Modern Infectious Disease Epidemiology: Concepts, Methods, Mathematical Models, and Public Health*, edited by A. Krämer, M. Kretzschmar, and K. Krickeberg (Springer New York, 2010) pp. 209–221.
[23] J. Hofbauer and K. Sigmund, *Evolutionary Games and Population Dynamics* (Cambridge University Press, 1998).
[24] M. H. Mohd, Diversity in interaction strength promotes rich dynamical behaviours in a three-species ecological system, Appl. Math. Comput. **353**, 243 (2019).
[25] C. Rackauckas and Q. Nie, Differentialequations.jl–a performant and feature-rich ecosystem for solving differential equations in julia, J. Open Res. Softw. **5** (2017).

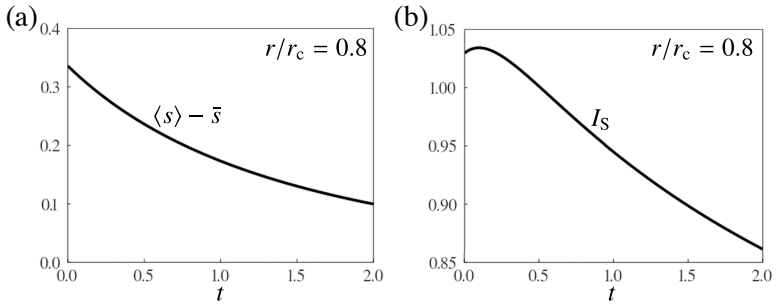

Supplementary Figure 1. **Typical time dependence of averaged quantities in the evolutionary model with natural selection and mutation.** Time dependence of (a) the average growth rate $\langle s \rangle$ and (b) the Shannon entropy I_S for the same parameters used in Figs. 2(a) and (b).

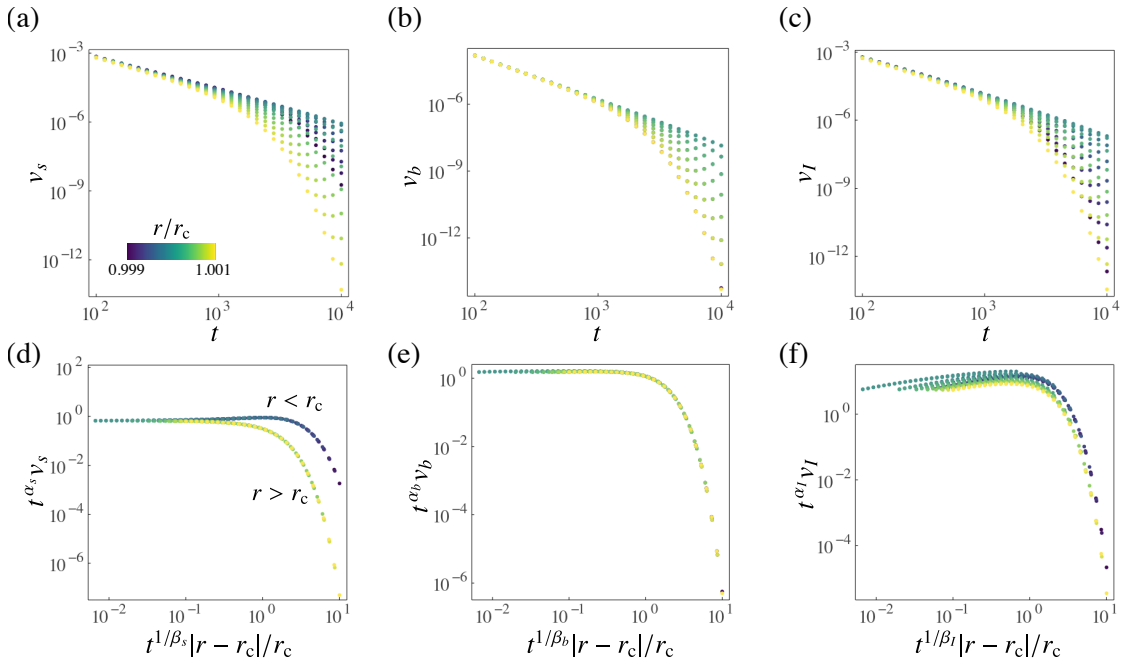

Supplementary Figure 2. **Dynamical scaling for the speeds of different quantities at the transcritical bifurcation.** Time and parameter dependence of the speeds (a) v_s, (b) v_b, and (c) v_I around the transcritical bifurcation point ($0.999 \leq r/r_c \leq 1.001$) of the evolutionary model with selection and mutation. (d-f) The corresponding scaling plots are shown with $\alpha_s = 3/2$, $\alpha_b = \alpha_I = 2$, and $\beta_s = \beta_b = \beta_I = 1$. Note that $v_b(r - r_c, t)$ seems to be almost independent of the sign of $r - r_c$ in the shown parameter regime. Also, $v_I(r - r_c, t)$ does not satisfy the scaling law due to the logarithmic time dependence at $r = r_c$ (i.e., $v_I \sim t^{-2} \ln t$). For all figures, we used the same parameters as those for Fig. 3(b).

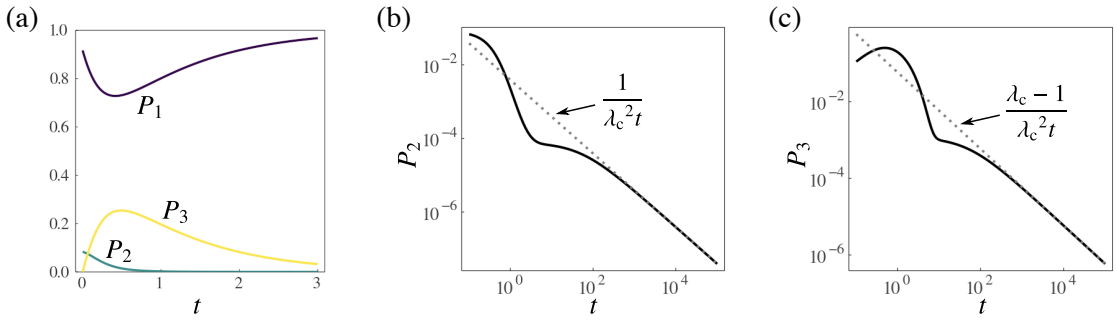

Supplementary Figure 3. **Typical time dependence of the proportion at the transcritical bifurcation point of the SIR model.** (a) Time dependence of the proportion in a short timescale. Long-time decay of the proportions of (b) the infected individuals and (c) the recovered individuals. In (b) and (c), the asymptotic forms [$P_2 \simeq (\lambda_c{}^2 t)^{-1}$ and $P_3 \simeq (\lambda_c - 1)(\lambda_c{}^2 t)^{-1}$] are shown with dotted lines (see Supplementary Method 4 for the derivation). For all figures, we used the same parameters as those for Fig. 3(d).

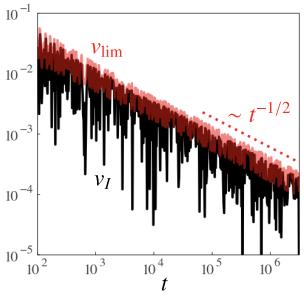

Supplementary Figure 4. **Power-law decay of the speed of change in diversity at the supercritical Hopf bifurcation.** We plot the time dependence of v_I (black line) and v_{lim} (red line) at the Hopf bifurcation point of the competitive Lotka-Volterra model. The asymptotic form ($v_{\mathrm{lim}} \sim t^{-1/2}$) is shown with a dotted line. We used the same parameters as those for Fig. 4(c).

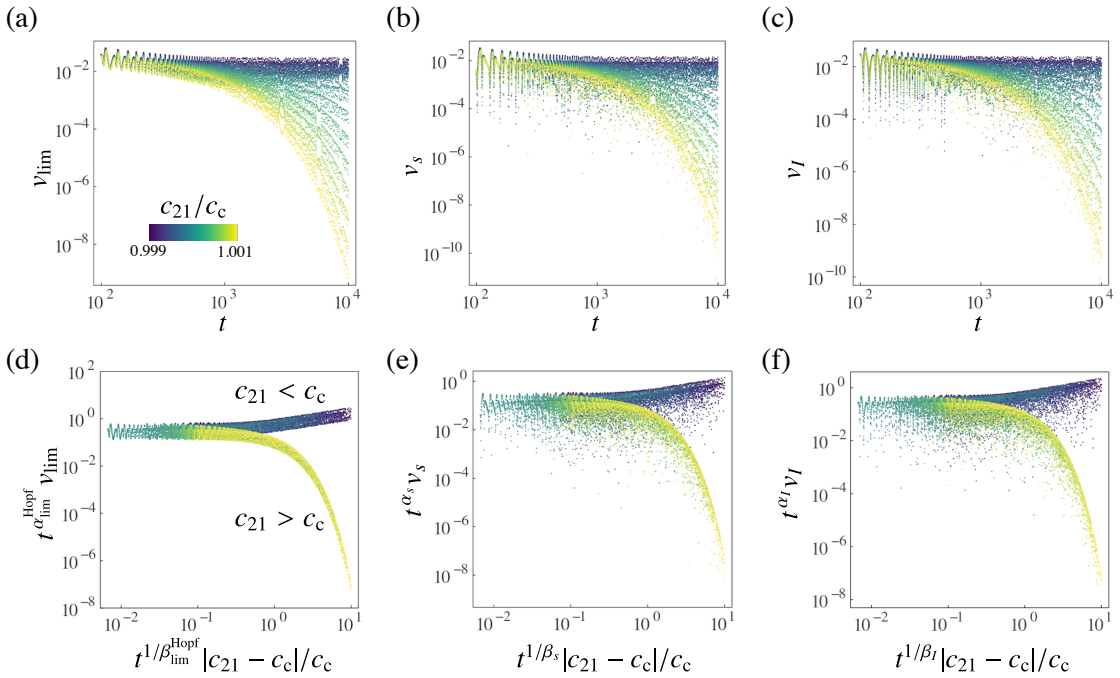

Supplementary Figure 5. **Dynamical scaling for speeds of different quantities at the supercritical Hopf bifurcation.** Time and interaction dependence of (a) the speed limit $v_{\rm lim}$ and the speeds (b) v_s and (c) v_I around the Hopf bifurcation point of the competitive Lotka-Volterra model. (d-f) The corresponding scaling plots are shown with $\alpha^{\rm Hopf}_{\rm lim} = \alpha_s = \alpha_I = 1/2$ and $\beta^{\rm Hopf}_{\rm lim} = \beta_s = \beta_I = 1$. In (d), the same data as plotted in Fig. 4(d) are reproduced for completeness. The amplitudes of oscillating $v_{\rm lim}$, v_s, and v_I follow the scaling laws. See Supplementary Method 6 for the parameters used.